

The POWHEG BOX

C. Oleari^a

^aDipartimento di Fisica "G. Occhialini" and INFN, Sezione di Milano-Bicocca, Università di Milano-Bicocca, 20126 Milano, Italy

We review the key features of POWHEG, a method for interfacing parton-shower Monte Carlo generators to fixed next-to-leading order QCD computations. We describe a recently introduced framework, the POWHEG BOX, that allows the automatic POWHEG implementation of any given NLO calculation. We present a few results for Higgs boson production via vector boson fusion and $Z + 1$ jet production, both processes available in the POWHEG BOX.

1. The POWHEG method

In the past two decades, next-to-leading order (NLO) QCD computations have become standard tools for phenomenological studies at lepton and hadron colliders. QCD tests have been mainly performed by comparing NLO results with experimental measurements, with the latter corrected for detector effects.

On the experimental side, leading order (LO) calculations, implemented in the context of general purpose Shower Monte Carlo (SMC) programs, have been the main tools used in the analysis. SMC programs include dominant QCD effects at the leading logarithmic level, but do not enforce NLO accuracy. These programs were routinely used to simulate background processes and signals in physics searches. When a precision measurement was needed, to be compared with a NLO calculation, one could not directly compare the experimental output with the SMC output, since the SMC does not have the required accuracy. The SMC output was used, in this case, to correct the measurement for detector effects, and the corrected result was compared to the NLO calculation.

In view of the positive experience with QCD tests at the NLO level, it has become clear that SMC programs should be improved, when possible, with NLO results. In this way a large amount of the acquired knowledge on QCD corrections would be made directly available to the experimentalists in a flexible form that they could easily use for simulations.

The problem of merging NLO calculations with parton shower simulations is basically that of avoiding overcounting, since the SMC programs do implement approximate NLO corrections already.

The features implemented in POWHEG can be summarized as follows:

- infrared-safe observables have NLO accuracy;
- collinear emissions are summed at the leading-logarithmic level;
- the double logarithmic region (i.e. soft and collinear gluon emission) is treated correctly if the SMC code used for showering has this capability.

In the case of HERWIG [1,2] this last requirement is satisfied, owing to the fact that its shower is based upon an angular-ordered branching.

In ref. [3] a method, called POWHEG (for Positive Weight Hardest Emission Generator), was proposed that produces positive-weighted events, and that is not SMC specific. In the POWHEG method the hardest radiation is generated first using the exact NLO matrix elements. The POWHEG output can then be interfaced to any SMC program that is either p_T -ordered, or allows the implementation of a p_T veto.¹ However, when interfacing POWHEG to angular-ordered SMC programs,

¹All SMC programs compatible with the *Les Houches Interface for User Processes* [4] should comply with this requirement.

the double-log accuracy of the SMC is not sufficient to guarantee the double-log accuracy of the whole result. Some extra soft radiation (technically called vetoed-truncated shower in ref. [3]) must also be included in order to recover double-log accuracy. In fact, angular ordered SMC programs may generate soft radiation before generating the radiation with the largest p_T , while POWHEG generates it first. When POWHEG is interfaced to shower programs that use transverse-momentum ordering, the double-log accuracy should be correctly retained if the SMC is double-log accurate. The ARIADNE program [5] and PYTHIA 6.4 [6] (when used with the new showering formalism), both adopt transverse-momentum ordering, in the framework of dipole-shower algorithm, and aim to have accurate soft resummation approaches, at least in the limit of large number of colours.

In the POWHEG formalism [7], the generation of the hardest emission is performed first, according to the distribution

$$d\sigma = \bar{B}(\Phi_B) d\Phi_B \left[\Delta(p_T^{\min}) + \frac{R(\Phi_R)}{B(\Phi_B)} \Delta(k_T(\Phi_R)) d\Phi_{\text{rad}} \right], \quad (1)$$

where $B(\Phi_B)$ is the leading order Born contribution and

$$\bar{B}(\Phi_B) = B(\Phi_B) + \left[V(\Phi_B) + \int d\Phi_{\text{rad}} R(\Phi_R) \right] \quad (2)$$

is the NLO differential cross section used to generate the Born variables ($V(\Phi_B)$ and $R(\Phi_R)$ stand respectively for the virtual and the real corrections), and

$$\Delta(p_T) = \exp \left[- \int d\Phi_{\text{rad}} \frac{R(\Phi_R)}{B(\Phi_B)} \theta(k_T(\Phi_R) - p_T) \right] \quad (3)$$

is the POWHEG Sudakov form factor. The transverse momentum of the emitted particle is here indicated with $k_T(\Phi_R)$. The cancellation of soft and collinear singularities is understood in the expression within the square bracket in eq. (2). Partonic events with hardest emission generated

according to eq. (1) are then showered with a k_T -veto on following emissions. For all the technicalities concerning this and other issues, we refer to [3,7].

Up to now, the POWHEG method, in the context of hadron colliders, has been applied to ZZ pair hadroproduction [8], heavy-flavour production [9], Drell-Yan vector boson production [10, 11], Higgs boson production via gluon fusion [12, 13], Higgs boson production associated with a vector boson (Higgs-strahlung) [13], single-top production [14], Higgs boson production in vector boson fusion [15] and $Z + 1$ jet production [16].

2. The POWHEG BOX

The POWHEG BOX [17] is a computer framework that implements in practice the theoretical construction of POWHEG. The aim of the POWHEG BOX is to construct a POWHEG implementation of a NLO process, given the following ingredients:

1. The list of all flavour structures of the Born processes.
2. The list of all flavour structures of the real processes.
3. The Born phase space.
4. The Born squared amplitudes \mathcal{B} , the color correlated ones \mathcal{B}_{ij} and spin correlated ones $\mathcal{B}_{\mu\nu}$. These are common ingredients of NLO calculations performed with a subtraction method.
5. The real matrix elements squared for all relevant partonic processes.
6. The finite part of the virtual corrections computed in dimensional regularization or in dimensional reduction.
7. The Born colour structures in the limit of a large number of colours.

With the exception of the virtual corrections, all these ingredients are nowadays easily obtained. A matrix element program can be used to obtain (4) and (5). The colour-correlated and

spin-correlated Born amplitudes can also be generated automatically. Recent progress in the automatization of the virtual cross section calculation may lead to developments where even the virtual contribution (6) may be obtained in a painless way. Given the ingredients listed above, the POWHEG BOX does all the rest. It automatically finds all the singular regions, builds the soft and collinear counterterms and the soft and collinear remnants, and then generates the radiation using the POWHEG Sudakov form factor.

3. Higgs boson production in vector-boson fusion

Higgs boson production via vector-boson fusion (VBF) is expected to provide a copious source of Higgs bosons in pp -collisions at the Large Hadron Collider (LHC) at CERN. It can be visualized as the inelastic scattering of two quarks (antiquarks), mediated by t -channel W or Z exchange, with the Higgs boson radiated off the weak bosons. It represents (after gluon fusion) the second most important production process for Higgs boson studies [18,19]. Once the Higgs boson has been found and its mass determined, the measurement of its couplings to gauge bosons and fermions will be of main interest [20,21]. Here VBF will play a central role since it will be observed in the $H \rightarrow \tau\tau$ [22,23], $H \rightarrow WW$ [24,25] and $H \rightarrow \gamma\gamma$ [26] channels. This multitude of channels allows to probe the different Higgs boson couplings. In addition, in order to distinguish the VBF Higgs boson signal from backgrounds, stringent cuts are required on the Higgs boson decay products as well as on the two forward quark jets which are characteristic for VBF. The efficiency of these cuts has to be evaluated on the basis of the most updated simulation tools and experimental inputs.

An additional feature characterizing VBF Higgs boson production is the fact that, at leading order, no colored particle is exchanged in the t channel so that no t -channel gluon exchange is possible at NLO, once we neglect the small contribution due to equal-flavour quark scattering with $t \leftrightarrow u$ channel interference. The different gluon radiation pattern expected for Higgs bo-

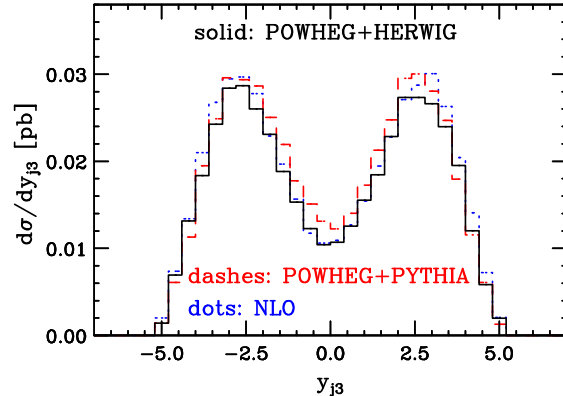


Figure 1. Rapidity y_{j3} of the third hardest jet, i.e. the one with highest p_T after the two tagging jets.

son production via VBF compared to its major backgrounds ($t\bar{t}$ production, QCD $WW + 2$ jet and QCD $Z + 2$ jet production) is at the core of the central-jet veto proposal, both for light [25] and heavy [27] Higgs boson searches. A veto of any additional jet activity in the central-rapidity region is expected to suppress the backgrounds more than the signal, because the QCD backgrounds are characterized by quark or gluon exchange in the t -channel. The exchanged partons, being colored, are expected to radiate off more gluons.

For the analysis of the Higgs boson coupling to gauge bosons, Higgs boson + 2 jet production via gluon fusion may also be treated as a background to VBF. When the two jets are separated by a large rapidity interval, the scattering process is dominated by gluon exchange in the t -channel. Therefore, like for the QCD backgrounds, the bremsstrahlung radiation is expected to occur everywhere in rapidity. An analogous difference in the gluon radiation pattern is expected in $Z + 2$ jet production via VBF fusion versus QCD production [28]. In order to analyze this feature, we have plotted in fig. 1 the rapidity of the third jet, the one with highest p_T after the two tagging

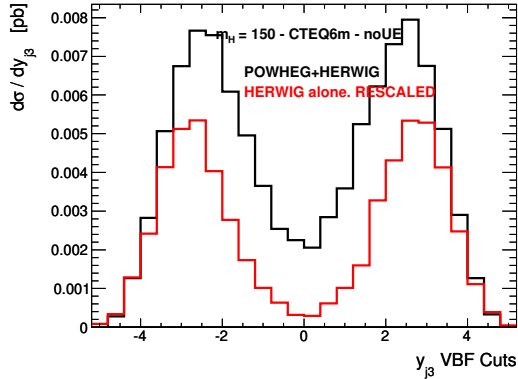


Figure 2. Comparison between the rapidity distribution of the third jet, y_{j3} , obtained using POWHEG followed by the shower of HERWIG (in black), and HERWIG alone (in dark grey). The two curves have been normalised such that the total cross sections agree at NLO level.

jets. The conclusion that can be drawn from the figure is that the third jet in VBF prefers to be emitted close to one of the tagging jets, while, in gluon fusion, it is emitted anywhere in the rapidity region between the tagging jets. Thus, at least with regard to the hard radiation of a third jet, the analysis of refs. [29,30,31] is confirmed. The distributions, obtained using POWHEG interfaced to HERWIG and PYTHIA, are very similar and turn out to be well modeled by the respective distributions of the NLO jet.

For comparison, in figs. 2 and 3 we have plotted the same distribution as obtained with HERWIG and PYTHIA alone. Both the two plots are normalized such that the total cross section is correct at NLO. In fig. 2, it is clear that the third jet produced by HERWIG underestimates the actual third-jet rapidity, even if the shape is similar. PYTHIA has instead a completely different behavior: here not only the normalization is wrong, but the predicted y_{j3} distribution is not correct. This is of no surprise, since both HERWIG and PYTHIA produce (and resum) correctly only jets in the collinear region (collinear with respect to the two tagging

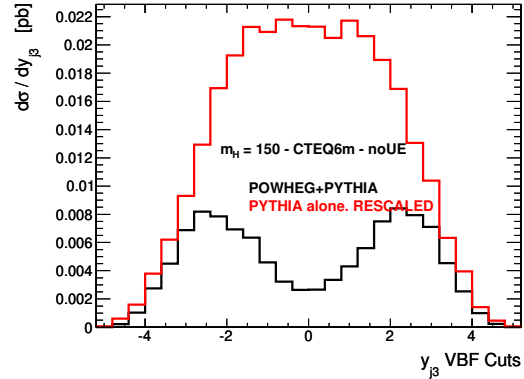


Figure 3. Comparison between the rapidity distribution of the third jet, y_{j3} , obtained using POWHEG followed by the shower of PYTHIA (in black), and PYTHIA alone (in dark grey). The two curves have been normalized such that the total cross sections agree at NLO level.

jets), so that we do not expect any distribution involving the third jet to be correct.

4. $Z + 1$ jet production

In the early LHC phase, $Z + 1$ jet production is a promising process for jet calibration. Both Z and W production in association with jets are important sources of missing energy signals, and W in association with jets is an important background to many new physics searches. The Z production process, with the Z decaying into leptons, gives a distinct signature that allows to perform stringent tests of the production mechanism. These tests have been performed extensively at the Tevatron, both at CDF [32] and at D0 [33,34,35,36]. They are carried out by correcting the measured quantities to the particle level, according to the recommendations developed in the 2007 Les Houches workshop [37], and then compared to NLO theoretical calculations, corrected for showering and underlying event effects. These corrections, in turn, are extracted from SMC programs.

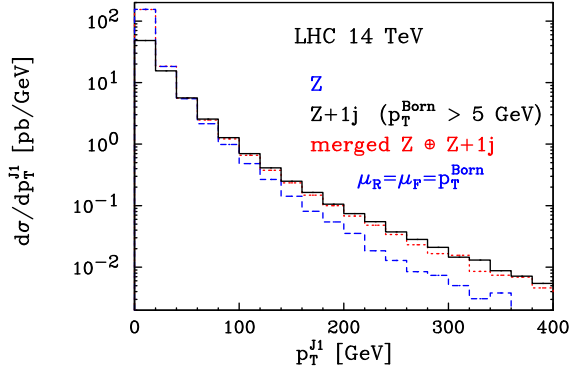


Figure 4. The p_T distribution of the first jet, in single Z production (blue dashed curve), in $Z + 1$ jet production (black solid curve) and of the merged sample (red dotted curve).

Very recently we have implemented $Z + 1$ jet in the POWHEG BOX. As a matter of fact, the POWHEG BOX framework was developed with the $Z + 1$ jet process as its first example process. It is clear that, by using this tool, the comparison of the theoretical prediction with the experimental results is eased considerably, and is also made more precise. Rather than estimating shower and underlying event corrections, using a parton shower program, these corrections can now be applied directly to the hard process in question, yielding an output that can be compared to the experimental results at the particle level. We have carry out this task and compared our results to the Tevatron findings. We remark, however, that a further improvement to this study could be carried out, by using the POWHEG program to generate the events that are fed into the detector simulation, and are directly compared to raw data. We are not, of course, in a position to perform such a task, that should instead be carried out by the experimental collaborations.

Since a POWHEG implementation of Z production has already appeared in the literature [10], a natural question arises, weather we can now, with the new $Z + 1$ jet calculation, build a merged

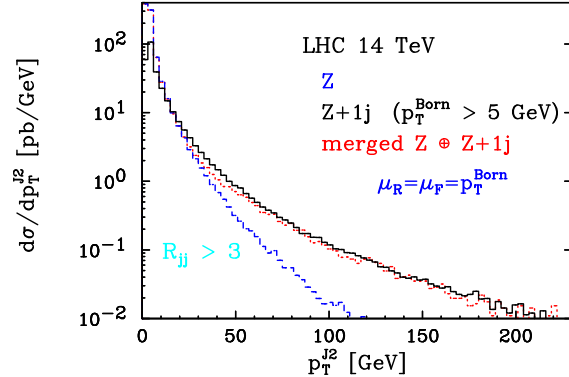


Figure 5. The p_T distribution of the second jet, in single Z production (blue dashed curve), in $Z + 1$ jet production (black solid curve) and of the merged sample (red dotted curve), when an angular separation $R_{jj} > 3$ is imposed between the two leading jets.

sample of the two programs, capable of describing Z production in the low, as well as in the high transverse-momentum region. We have presented, for the first time, a minimalistic approach to such a merging, by putting together independent samples of Z and $Z + 1$ jet events in the most straightforward way, described in details in a forthcoming paper [16].

In fig. 4 we have plotted the p_T distribution of the first jet, in single Z production (blue dashed curve), in $Z + 1$ jet production (black solid curve) and of the merged sample (red dotted curve). As can be seen in the figure, the merged distribution smoothly interpolates between the single Z behavior at small p_T , where the Sudakov form factor plays an important role in resumming the divergent collinear singularities, and the $Z + 1$ jet curve, at high p_T , where the presence of the second hard jet in the $Z + 1$ jet sample, hardens the distribution of the first jet. Similar interpolating behavior is seen for the p_T of the second jet, in fig. 5. Here, an angular separation $R_{jj} > 3$ is imposed between the two leading jets, in order to separate them further to better illustrate the

behavior of the merged curve.

5. Acknowledgments

The results presented in this talk have been obtained in collaboration with S. Alioli, P. Nason and E. Re.

REFERENCES

1. G. Corcella et al., JHEP 01 (2001) 010, hep-ph/0011363.
2. G. Corcella et al., (2002), hep-ph/0210213.
3. P. Nason, JHEP 11 (2004) 040, hep-ph/0409146.
4. E. Boos et al., (2001), hep-ph/0109068.
5. L. Lonnblad, Comput. Phys. Commun. 71 (1992) 15.
6. T. Sjostrand, S. Mrenna and P. Skands, JHEP 05 (2006) 026, hep-ph/0603175.
7. S. Frixione, P. Nason and C. Oleari, JHEP 11 (2007) 070, 0709.2092.
8. P. Nason and G. Ridolfi, JHEP 08 (2006) 077, hep-ph/0606275.
9. S. Frixione, P. Nason and G. Ridolfi, JHEP 09 (2007) 126, 0707.3088.
10. S. Alioli et al., JHEP 07 (2008) 060, 0805.4802.
11. K. Hamilton, P. Richardson and J. Tully, JHEP 10 (2008) 015, 0806.0290.
12. S. Alioli et al., JHEP 04 (2009) 002, 0812.0578.
13. K. Hamilton, P. Richardson and J. Tully, JHEP 04 (2009) 116, 0903.4345.
14. S. Alioli et al., JHEP 09 (2009) 111, 0907.4076.
15. P. Nason and C. Oleari, JHEP 02 (2010) 037, 0911.5299.
16. S. Alioli et al., to appear soon.
17. S. Alioli et al., JHEP 06 (2010) 043, 1002.2581.
18. CMS Collaboration, Report CMS/LHCC/2006-021, CMS TDR 8.2.
19. ATLAS Collaboration, Report CERN/LHCC/99-15 (1999).
20. D. Zeppenfeld et al., Phys. Rev. D62 (2000) 013009, hep-ph/0002036.
21. M. Dührssen et al., Phys. Rev. D70 (2004) 113009, hep-ph/0406323.
22. D.L. Rainwater, D. Zeppenfeld and K. Hagiwara, Phys. Rev. D59 (1999) 014037, hep-ph/9808468.
23. T. Plehn, D.L. Rainwater and D. Zeppenfeld, Phys. Rev. D61 (2000) 093005, hep-ph/9911385.
24. D.L. Rainwater and D. Zeppenfeld, Phys. Rev. D60 (1999) 113004, hep-ph/9906218.
25. N. Kauer et al., Phys. Lett. B503 (2001) 113, hep-ph/0012351.
26. D.L. Rainwater and D. Zeppenfeld, JHEP 12 (1997) 005, hep-ph/9712271.
27. V.D. Barger, R.J.N. Phillips and D. Zeppenfeld, Phys. Lett. B346 (1995) 106, hep-ph/9412276.
28. D.L. Rainwater, R. Szalapski and D. Zeppenfeld, Phys. Rev. D54 (1996) 6680, hep-ph/9605444.
29. V. Del Duca, A. Frizzo and F. Maltoni, JHEP 05 (2004) 064, hep-ph/0404013.
30. V. Del Duca et al., JHEP 10 (2006) 016, hep-ph/0608158.
31. J.R. Andersen, V. Del Duca and C.D. White, JHEP 02 (2009) 015, 0808.3696.
32. CDF - Run II, T. Aaltonen et al., Phys. Rev. Lett. 100 (2008) 102001, 0711.3717.
33. D0, V.M. Abazov et al., Phys. Lett. B658 (2008) 112, hep-ex/0608052.
34. D0, V.M. Abazov et al., Phys. Lett. B669 (2008) 278, 0808.1296.
35. D0, V.M. Abazov et al., Phys. Lett. B678 (2009) 45, 0903.1748.
36. D0, V.M. Abazov et al., Phys. Lett. B682 (2010) 370, 0907.4286.
37. C. Buttar et al., (2008), 0803.0678.